

## Evolution of III-V Nitride Alloy Electronic Structure: The Localized to Delocalized Transition

P. R. C. Kent and Alex Zunger

National Renewable Energy Laboratory, Golden, Colorado 80401

(Received 25 September 2000)

Addition of nitrogen to III-V semiconductor alloys radically changes their electronic properties. We report large-scale electronic structure calculations of GaAsN and GaPN using an approach that allows arbitrary states to emerge, couple, and evolve with composition. We find a novel mechanism of alloy formation where localized cluster states within the gap are gradually overtaken by a downwards moving conduction band edge, composed of both localized and delocalized states. This localized to delocalized transition explains many of the hitherto puzzling experimentally observed anomalies in III-V nitride alloys.

DOI: 10.1103/PhysRevLett.86.2613

PACS numbers: 71.55.Eq, 71.15.-m

Random substitution of impurity atoms onto the atomic sites of a host crystal creates a statistical distribution of isolated impurities, impurity pairs, triplets, etc. This distribution of different sized clusters reflects the fluctuations inherent to the disordered states. In *conventional* isovalent semiconductor alloys [1] (Si-Ge, GaP-InP, AlAs-InAs), characterized by a small difference in the properties (electronegativity, atomic size, and potential offset) of the host and impurity atoms, such impurity clusters do not create bound electronic levels in the fundamental band gap. Instead, these “cluster states” (CS) appear as weak resonances *within* the valence or conduction band continua, where they hybridize with the host crystal states. The “perturbed host states” (PHS) remain delocalized and retain an approximate translational symmetry, in that their projection on periodic Bloch states peaks at a well-defined “majority representation” [2] wave vector. As the impurity concentration increases, one observes a *continuous change* in the band gap (“optical bowing”), effective masses, pressure deformation potentials, and interband transition energies. Such alloy states cannot be described theoretically by approaches that altogether ignore the random fluctuations and the ensuing cluster states, e.g., the “virtual crystal approximation” [1], the “coherent potential approximation” [1], the “two-level anticrossing model” [3],  $k \cdot p$  alloy models [4], or modeling the alloys as small “supercells” containing an *ordered* array of impurities [5].

In contrast to weakly perturbed alloy systems, one encounters a special group of isovalent alloys where the differences in properties of the host and impurity atoms are large enough that even *isolated* impurities create bound states in or near the fundamental band gap [6,7]. In such alloy systems (ZnS:Te, GaP:N, GaAs:N, GaN:As) the CS appear *within* the fundamental band gap, as a progression of narrow energy levels [6] associated with single impurities, impurity pairs, triplets, etc., whereas the PHS appear as sharp resonances (“virtual bound states”) within the continua. Such alloy systems lack “majority representation” [2] wave vectors, as Bloch symmetry is lost. Since such strongly perturbing impurities introduce fundamentally new electronic levels (rather than modified host

levels), the alloy properties do not manifest a gradual and smooth evolution with composition. Instead, one observes in the dilute “impurity limit” of, e.g., GaAs<sub>1-x</sub>N<sub>x</sub>, GaP<sub>1-x</sub>N<sub>x</sub>, a progression of sharp emission lines [6–11], unusually large band-edge effective masses [12], and small pressure deformation potentials [9,13,14]. As the impurity concentration increases, the energies of the sharp lines remain at first fixed [11,15,16], and then the lines mysteriously disappear, one by one [11,15,16], as the effective mass reaches a maximum [12]. As the composition is increased further, the emission turns into a broad band [11,15,17] which has a rapid redshift vs composition (band gap bowing of  $\sim 20$  eV in GaAsN) [5], an anomalously low temperature coefficient [10], and a peculiar saturation of the energy with applied pressure [3]. Such alloys cannot be described by models that neglect fluctuations [1] or multiband coupling [3,4].

We have developed a pseudopotential supercell technique [2] suitable for modeling strongly perturbed fluctuating alloys. A random alloy is described as a large (1000–14 000 atom) box of the host crystal onto which an arbitrary number of impurity atoms are randomly substituted, thus creating a natural statistical distribution of various impurity clusters [2]. Atomic positions are relaxed (via a classic force field) to their strain minimizing positions. The electronic structure of several randomly selected configurations is computed via an empirical pseudopotential approach, after applying (artificial) periodicity to the large box. This approach describes the evolution of alloy states in an unbiased manner as alloy fluctuations are fully retained. Furthermore, specific CS and PHS are not assumed [3], but emerge naturally; such states are permitted to interact and evolve with composition. Here we apply this approach to GaP<sub>1-x</sub>N<sub>x</sub> and GaAs<sub>1-x</sub>N<sub>x</sub>, investigating how the discrete CS, located initially in the fundamental band gap, and the PHS located within the continua develop with composition. We find that (i) the CS located in the band gap do not interact sufficiently so as to broaden and form an “impurity band” made of a superposition of such nitrogen-induced states [12]. Instead, the energy of the CS remains relatively constant, while the PHS broaden,

move down in energy into the fundamental band gap, and overtake the CS one by one. (ii) Once the CS are swept by the PHS, the ensuing “amalgamation of states” forming the conduction band-edge exhibits *alloy fluctuations*, as its low-energy tail is dominated by the just swept-in CS, whereas its higher-energy end consists of the more extended PHS. This localized-delocalized duality in the band edge leads to exciton localization in the tail states, Stokes shift between absorption (into PHS) and emission (from CS), blueshift of low-temperature photoluminescence (PL) with increasing temperature (due to thermal transfer of carriers from CS to PHS), and anomalous pressure dependence of the band gap (due to the weak pressure dependence of the CS, at the band edge, compared to the bulk). (iii) As the impurity concentration increases further, the amalgamated band-edge state broadens, the states delocalize, and the system turns into a conventional alloy with smoothly varying physical properties. These nitride systems thus illustrate a novel class of alloy behavior, which we predict to be common to other isoelectronic systems [6,7] where localized CS occur.

The calculated 20-40 near-gap eigenstates for each of 15 random configurations, e.g.,  $\text{Ga}_{500}\text{As}_{500-m}\text{N}_m$ , per composition  $x = m/500$ , are analyzed by monitoring their energies, pressure dependence, and localization. The latter is characterized by their projection on Bloch-periodic states, and by calculating the distance  $R_\alpha^{(i)}$  from the  $\alpha$ th nitrogen site at which 20% of the amplitude of eigenstate  $\psi_i$  is enclosed. Figure 1 depicts the spectral dependence of the average localization  $\sum_\alpha 1/R_\alpha^{(i)}$  for nitrogen-localized CS and for the quasilocalized PHS in  $\text{GaAs}_{1-x}\text{N}_x$ .

*Ultradilute limit.*—We start in Figs. 1a and 1b with the ultradilute limit where nitrogen impurities are *isolated* and do not interact with other nitrogens. To study this limit we place a *single* substitutional nitrogen in a 13 824 atom cell, then separately, single nitrogen pairs  $\text{NN}_m$  whose atoms are  $m$ th nearest neighbors, then separately a nitrogen  $\text{NN}_\alpha\text{N}_\beta$  triplet forming a “ $\text{Ga}(\text{AsN}_3)$ ” cluster with three nitrogens and one arsenic surrounding a common gallium atom, and separately a  $\text{GaN}_4$  cluster. We find that the valence states are comparatively weakly perturbed, so show just the conduction states.

For the *isolated impurity* we find that a strong, nitrogen-mediated coupling of the host crystal band-edge states [8] creates  $a_1$ -like impurity-induced states  $a_1(1)$ ,  $a_1(2)$ ,  $a_1(3)$ , and  $a_1(4)$  from the basis  $a_1(X_{1c}) + a_1(L_{1c}) + a_1(\Gamma_{1c}) + a_1(N)$ . The wave functions of these  $\text{GaAs:N}$  impurity-induced  $a_1$  states are depicted in Fig. 2, showing clear noneffective mass behavior. The lowest-energy  $a_1^{\Gamma L}(1)$  state forms the bottom of the PHS, whereas the  $a_1^{\Gamma L}(3)$  is its counterpart with reverse proportions of  $\Gamma$  and  $L$ . Both states exhibit some nitrogen localization (Figs. 2a and 2c). Between these states we find the highly nitrogen-localized  $a_1^N(2)$  level (Fig. 2b), composed of many high-energy bulk states from throughout the Brillouin zone, at  $E_c + 150$  meV, in good agreement with the 150–180 meV

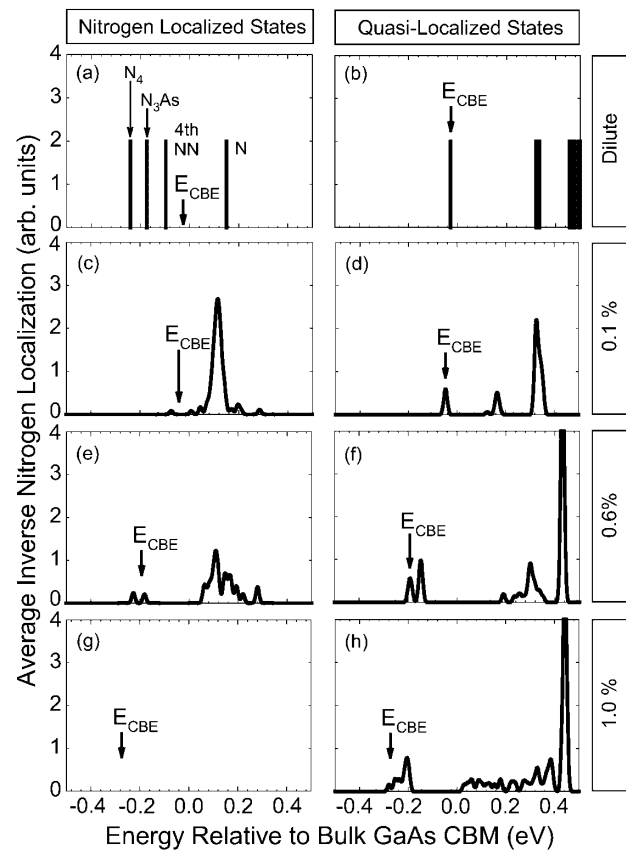


FIG. 1. Spectral dependence of average nitrogen localization for (left) nitrogen-localized “cluster states” and (right) quasi-localized “perturbed host states” of  $\text{GaAsN}$  for a few nitrogen concentrations. States with at least 20% of total charge within  $4.1 \text{ \AA}$  radius of any nitrogen atom are classified as nitrogen localized. The vertical arrows show the position of the alloy conduction band edge  $E_{\text{CBE}}$ . For the dilute limit we show the energies of several illustrative cluster states: a quadruplet ( $\text{N}_4$ ), triplet ( $\text{AsN}_3$ ), 4th neighbor pair (4th NN), and the isolated impurity level ( $\text{N}$ ).

measured experimentally [13,18], where  $E_c$  denotes the *bulk*  $\text{GaAs}$  conduction band minimum (CBM) energy. Moreover, we find that at a pressure of  $\sim 2$  GPa, this level crosses the  $a_1^{\Gamma L}(1)$  CBM, thus becoming the lowest level in the gap, in excellent agreement with hydrostatic pressure measurements [13,18].

As *impurity pairs* are created, the states of isolated nitrogen form bonding-antibonding pairs, with strong lattice relaxation leading to a progression of highly localized states in the gap (Fig. 1a). In the dilute  $\text{GaAs:N}$  limit we find 1st and 4th neighbor pairs with levels  $\sim E_c - 100$  meV, whereas other pairs form resonances *inside* the conduction band. When we apply the same calculation to In-In pairs in  $\text{GaAs}$ , no gap states are created, highlighting the uniqueness of the  $\text{GaAsN}$ ,  $\text{GaPN}$  systems. The  $\text{Ga}(\text{AsN}_3)$  triplet gives rise to a level at  $E_c - 175$  meV and the  $\text{GaN}_4$  quadruplet gives  $E_c - 240$  meV. The highly nitrogen-localized wave functions of pairs and clusters are shown in Fig. 3a. Because of their low concentrations,

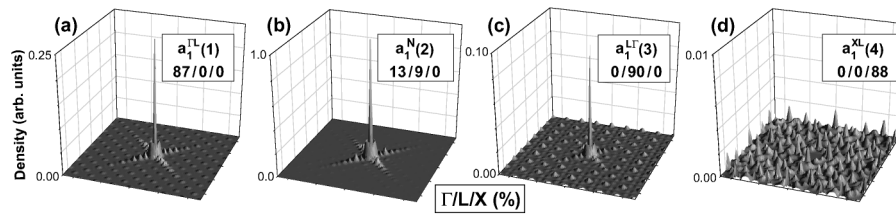


FIG. 2. Wave functions of the lowest energy  $a_1$  conduction states of GaAs:N ( $x_N \sim 0.05\%$ ). The  $x$  and  $y$  axes lie in the [100] and [010] directions, respectively.

high-order cluster states, spread throughout the upper part of the band gap hardly absorb light, but can be efficiently populated by tunneling from the higher-energy mobile PHS occupied optically. Thus CS are seen in PL, even though their concentration is low. This creates a Stokes shift between absorption and emission [11]. Furthermore, deeper CS appear in PL as the temperature is raised [10], when these levels are fed by cascading from the thermally populated higher-energy mobile states. The calculated pressure dependence of the pairs and cluster states in GaAs is  $a_p = 20\text{--}60$  meV/GPa, while for the isolated N level  $a_p = 40$  meV/GPa. These values are much reduced relative to the  $\Gamma_{1c}$  bulk value of 100 meV/GPa due to mixing of  $X_{1c}$  and  $L_{1c}$  character with much reduced  $a_p$ .

Calculations for GaP:N show similar behavior when compared to GaAs:N (Fig. 1), except that in the ultralimit (a) the  $a_1(N)$  level is already inside the band gap at  $E_c - 30$  meV, compared with the measured [6,9,13,14]  $E_c - 36$  meV, and (b) the edge of the PHS is the indirect state  $e(X_{1c})$ , not  $a_1^{L\Gamma}(1)$  as in GaAsN. The cluster states are in the gap, e.g., the 4th neighbor pairs at  $E_c - 167$  meV, the triplet and quadruplet cluster states at  $E_c - 196$  and  $E_c - 214$  meV, respectively. (c) All cluster states exhibit a pronounced mixing of  $\Gamma$  character, and are hence nominally “direct gap states” as noted experimentally [16]. (d) The pressure coefficients of pairs and triplets are in the range 20–40 meV/GPa, and the isolated impurity  $a_1^N$  state has  $a_p \approx 0$ . These values are smaller than in GaAsN due to the greater involvement of  $a_1(X_{1c})$  states in GaP with its attendant smaller  $a_p$ .

*Evolution as composition is increased.*—Figures 1c–1h depict the evolution of CS and PHS with alloy composition

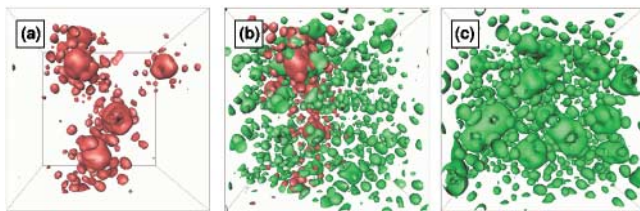


FIG. 3 (color). Isosurfaces of the conduction wave functions for (a)  $x \ll x_c$  GaAsN showing nitrogen-localized cluster states within the gap (red), (b)  $x \approx x_c$  showing the “amalgamated state” of localized (red) and the delocalized (Bloch-like) states (green), and (c)  $x \gg x_c$  extended states (green).

for GaAs $_{1-x}$ N. The vertical arrows show the position of the alloy conduction band minimum  $E_{CBE}$ , made of PHS (called  $E_-$  in [3]). The important features are as follows.

(i) The edge  $E_{CBE}$  of the PHS moves rapidly into the gap (with calculated band gap bowing coefficient  $b = 13$  and 20 eV [19] at 1% in GaP and GaAs, respectively), whereas the energies of the CS in the band gap are rather insensitive to the global composition  $x$ . This behavior reflects the strong localization of the band gap CS (cf. Fig. 2), compared with the more extended PHS which exhibit strong interband coupling and anticrossing.

(ii) The  $\Gamma$ -L-X interband couplings within the PHS have several effects. First, the coupling imparts  $\Gamma_{1c}$  character to the  $E_{CBE}$  states in indirect-gap GaP, making it direct gap, in agreement with observations [16]. Second, significant calculated  $L_{1c}$  character is introduced into the PHS, seen in resonant Raman scattering in GaAsN [20]. The calculated splitting between the  $a_1^\Gamma E_{CBE}$  and  $a_1^{L\Gamma}$  is about 0.5 eV at 1%, in excellent agreement with the 0.5 eV ballistic electron emission spectroscopy value [21]. Third, the high-energy side of the PHS exhibits the  $t_2(L_{1c})$  state at  $\sim E_c + 0.43$  eV, which stays rather constant as a function of  $x$  (since the  $t_2$  symmetry state has few matching impurity levels to couple with at these energies). Transitions into this  $t_2(L_{1c})$  state from the corresponding  $L_{1v}$  state in the valence band (at  $E_c - 2.5$  eV) thus exhibit negligible (but slightly positive)  $x$  dependence, as noted experimentally [14] for the  $L_{1v} \rightarrow L_{1c}$ -like “ $E_1$  transition” in GaAsN in the  $\sim 3$  eV spectral range.

(iii) The CS in the band gap are swept away, one by one, by the downward moving PHS. The last states to be swept are the deepest—the triplets and quadruplets. The critical composition  $x_c$  for the localized-to-delocalized transition depends on the short-range order in the alloy: in an ideal random alloy we estimate the transition occurs at  $x_c \sim 0.6\%$  for GaAsN and  $x_c \sim 2\%$  in GaPN (Fig. 1), whereas phase separation and clustering, short-range order reduces  $x_c$  (currently grown alloys seem to exhibit nonrandomness). The larger  $x_c$  in GaPN reflects the fact that the CS are deeper, reflecting that on an absolute energy scale the CBM of GaP is 0.3 eV higher [22] than that of GaAs.

(iv) Once the CS have just been swept away by the PHS,  $x \geq x_c$ , an amalgamation of states is formed at the band edge. Figure 3b shows the wave function for  $x \approx x_c$ . In contrast to  $x \ll x_c$  (Fig. 3a), now both localized (red) and delocalized (green) features appear. Such states (Fig. 3b)

exhibit alloy fluctuation: Its “localized low-energy” (LLE) edge is made up of a statistical distribution of CS-like levels, with different degrees of localization, and “delocalized high-energy” (DHE) states. This duality has a few consequences: First, near  $x_c$  the effective mass will be large [12], as many localized (heavy-mass) states make up the band edge. Second, exciton recombination at low temperature will be controlled by LLE states, consistent with the observed slow decay times [17], blueshift of PL with increased excitation power [17] (due to state filling of LLE states), rapid decrease of temperature coefficient of the band gap [10] (due to thermal depopulation of the LLE near-edge states), and Stokes shift between absorption (to DHE) and emission (from LLE). The increased mixing of localized CS with delocalized PHS affects the band gap  $a_p$ , found here for  $p \ll 1$  GPa in GaPN to increase linearly with  $x$  from 19 to 31 meV/GPa at 1%, 2%, respectively, in excellent agreement with recent measurements of GaPN [14] ( $\sim 19$  to  $\sim 30$  meV/GPa at 0.7%, 2%, respectively). The coefficient increases due to the increased proportion of pairs and clusters (strongly pressure dependent CS) to isolated impurities (weakly pressure dependent CS) with increasing  $x$ . In GaAsN the calculated pressure coefficient saturates with applied pressure reducing, for example, from  $\sim 68$  meV/GPa to  $\sim 28$  meV/GPa at 5 GPa for  $x = 2\%$ , compared with  $\sim 71$  meV/GPa to  $\sim 38$  meV/GPa at 5 GPa for 2.3% nitrogen InGaAsN samples [3]. The reduction in pressure coefficient results from the increased localization of states at the conduction band edge and their decoupling from delocalized host states.

(v) Once all CS have been swept away by PHS and are well inside the conduction band ( $x \gg x_c$ , Figs. 1h and 1g), conventional alloy behavior begins to emerge as the states become more delocalized. Figure 3c shows the now extended wave function. In this composition regime  $E_{\text{CBE}}$  is well below the CS, so the temperature dependence of the band gap is constant, as no thermal depopulation of LLE states is needed.

(vi) At  $x \geq 1\%$  we find a broader set of states at  $E_{\text{CBE}} + (0.5-0.7)$  eV which we term, in analogy with Ref. [3], the “ $E_+$ ” band. The energy of the band moves up with  $\sqrt{x}$ , as seen in Ref. [15]. However, while “ $E_-$ ” at the  $E_{\text{CBE}}$  is a localized band, “ $E_+$ ” in our calculation appears as a delocalized, host-perturbed band.

In summary, our calculations lead to the following physical picture for the evolution of alloy states in III-V nitrides: The alloys are distinguished from other isovalent III-V alloys by the occurrence in the dilute limit of an hierarchical distribution of different CS inside the band gap and PHS, resulting from strong multiband ( $\Gamma$ -L-X) coupling in the continuum of conduction states. As the alloy composition increases, the energies of the highly localized CS stay fixed, but the PHS move down in energy due to internal level repulsion, sweeping the fixed-energy CS one by one into the conduction band. This leads, at  $x_c$ , to an amalgamation of states at the band edge composed

of localized low-energy states developed from the CS, and delocalized states developed from the PHS. The localized-delocalized duality of the band edge leads to exciton localization, Stokes shift, blueshift of PL with temperature (at low temperatures) and increased excitation power. The “two-level anticrossing” model [3] neglects alloy fluctuations and thus the ensuing effects listed above. At the same time, this model phenomenologically fits the observed dependence of the band gap on composition, pressure, and temperature by assuming an effective (non-fluctuating) electronic state. We propose instead that the CS and the “amalgamated” conduction band edge found here naturally identify the experimentally observed states.

This work is supported by the U.S. Department of Energy, SC-BES-OER Grant No. DE-AC36-98-GO10337.

- 
- [1] A.B. Chen, *Semiconductor Alloys* (Plenum, New York, 1995); M. Jaros, *Deep Levels in Semiconductors* (Adam Hilger, Bristol, 1982).
  - [2] L.-W. Wang, L. Bellaiche, S.-H. Wei, and A. Zunger, *Phys. Rev. Lett.* **80**, 4725 (1998); L. Bellaiche, S.-H. Wei, and A. Zunger, *Phys. Rev. B* **54**, 17568 (1996).
  - [3] W. Shan *et al.*, *Phys. Rev. Lett.* **82**, 1221 (1999).
  - [4] A. Lindsay and E. P. O'Reilly, *Solid State Commun.* **112**, 443 (1999).
  - [5] A. Rubio and M.L. Cohen, *Phys. Rev. B* **51**, 4343 (1995); E.D. Jones *et al.*, *Phys. Rev. B* **60**, 4430 (1999); S.-H. Wei and A. Zunger, *Phys. Rev. Lett.* **76**, 664 (1996).
  - [6] J.J. Hopfield, D.G. Thomas, and R.T. Lynch, *Phys. Rev. Lett.* **17**, 312 (1966).
  - [7] W. Czajka, *Festkörperprobleme* **11**, 65 (1971).
  - [8] T. Mattila, S.-H. Wei, and A. Zunger, *Phys. Rev. B* **60**, R11245 (1999).
  - [9] B. Gil *et al.*, *Phys. Rev. B* **29**, 3398 (1984); M.I. Eremets *et al.*, *Semicond. Sci. Technol.* **4**, 267 (1989).
  - [10] H. Yaguchi *et al.*, *J. Cryst. Growth* **189/190**, 496 (1998); K. Uesugi *et al.*, *Appl. Phys. Lett.* **76**, 1285 (2000).
  - [11] T. Makimoto, H. Saito, T. Nishida, and N. Kobayashi, *Appl. Phys. Lett.* **70**, 2984 (1997).
  - [12] Y. Zhang, A. Mascarenhas, H.P. Xin, and C.W. Tu, *Phys. Rev. B* **61**, 7479 (2000).
  - [13] X. Liu, M.-E. Pistol, and L. Samuelson, *Phys. Rev. B* **42**, 7504 (1990).
  - [14] W. Shan *et al.*, *Phys. Rev. B* **62**, 4211 (2000).
  - [15] P.J. Klar *et al.*, *Appl. Phys. Lett.* **76**, 3439 (2000).
  - [16] H.P. Xin and C.W. Tu, *Appl. Phys. Lett.* **76**, 1267 (2000).
  - [17] I. Buyanova *et al.*, *Mater. Sci. Eng. B* **75**, 166 (2000).
  - [18] D.J. Wolford, J.A. Bradley, K. Fry, and J. Thompson, in *Proceedings of the 17th International Conference of the Physics of Semiconductors* (Springer, New York, 1984), p. 627.
  - [19] Thus, cluster states are not needed to explain large bowing.
  - [20] H.M. Cheong, Y. Zhang, A. Mascarenhas, and J.F. Geisz, *Phys. Rev. B* **61**, 13687 (2000).
  - [21] M. Kozhevnikov *et al.*, *Phys. Rev. B* **61**, R7861 (2000).
  - [22] R.G. Dandrea and A. Zunger, *Appl. Phys. Lett.* **57**, 1031 (1990).